Specificity of thermal stability and reactivity of two-dimensional layered Cu-Fe sulfide - Mg-based hydroxide compounds (valleriites)

Maxim Likhatski[a], Roman Borisov[a,b], Olga Fetisova[a], Anastasia Ivaneeva[a], Denis Karpov[a], Evgeny Tomashevich[a], Anton Karacharov[a], Sergey Vorobyev[a], Elena Mazurova[a], and Yuri Mikhlin[a]

[a] Institute of Chemistry and Chemical Technology, Krasnoyarsk Science Center of the Siberian Branch of the Russian Academy of sciences, Akademgorodok, 50/24, Krasnoyarsk, 660036, Russia

[b] Siberian Federal University, Svobodny av. 79, Krasnoyarsk, 660041, Russia

* Corresponding author (Maxim Likhatski, e-mail: lixmax@icct.ru)

Abstract

We recently synthesized prospective new materials composed of alternating quasi-atomic sheets of brucite-type hydroxide $(Mg,Fe)(OH)_2$ and $CuFe_{1-x}S_2$ sulfide (valleriites). Herein, their thermal behavior important for many potential applications has been studied in inert (Ar) and oxidative (20% O_2) atmosphere using TG and DSC analysis and characterization with XRD, XPS, SEM and EDX. In Ar media, the processes are determined by dehydroxylation of the hydroxide layers forming MgO, with the temperature of the major endothermic maximum of the mass loss at 413 °C. Sulfide sheets start to degrade below 500 °C and melt nearby 800 °C, with bornite, chalcopyrite and troilite specified as the final products. In oxidative atmosphere, the exothermic reactions with the mass increase peaked at 345 and 495 °C correspond to a partial and major oxidation of Cu-Fe sulfide layers, respectively. Sulfur oxides captured in magnesium hydroxide layers to form $MgSO_4$ compromised the layer integrity and promoted oxidation of the sulfide entities. The final products contained also minor MgO, Cu_2MgO_3, Fe_3O_4 and $MgFe_2O_4$ phases. Samples doped with Al, which decreases the content of Fe in hydroxide layers, show notably impeded decay of valleriite in argon but facilitated oxidation of Cu-Fe sulfides, while the impact of Li (it slightly increases the number of the Fe-OH sites) was less expressed. The mutual stabilization of the 2D hydroxide and sulfide layers upon heating in inert atmosphere but not in oxygen as compared with bulk brucite and chalcopyrite was suggested to explain by high thermal resistance across the stacked incommensurate sheets, which slows down the endothermic reactions and accelerates the exothermic oxidation; the high number of Fe atoms in the hydroxide sheets are expected to promote the phonon exchange and heat transfer between the layers.

Keywords: two-dimensional layered composite, valleriite, copper-iron sulfide, magnesium hydroxide, thermal analysis, DSC, thermal conductivity

1. Introduction

Two-dimensional (2D) materials, such as graphene, transition metal chalcogenides (MoS_2 and others) [1-3], nitrides and carbonitrides (MXenes) [4-7], hexagonal boron nitride (h-BN) [8,9], double layered hydroxides [10-12], and some others [13,14], attract great attention due to unique physical and chemical properties, which could be applied in electronics, catalysts, sensors, biomedicine and other fields. There exist also layered materials constructed by alternating quasi-atomic metal chalcogenide and hydroxide layers [15-20], first of all, FeSe and (Li,Fe)OH exhibiting superconductivity with the critical temperatures as high as 40 K [21-23], and unabundant natural minerals composed, in particular, of Fe sulfide (tochilinite) or Fe-Cu sulfide and Mg-based hydroxide (brucite) sheets (tochilinite and valleriite, respectively), and a series of rarer analogs of different composition [24, 25]. Valleriite $[(Fe^{3+},Cu^{+})S_2]\cdot x[(Mg,Fe,Al)(OH)_2\cdot]$ occurs in large amounts in the Noril'sk Cu-Ni ore provenance [26-28], largely in so-called cuprous ores, which remain uninvolved in industrial processing because of, among other reasons, poor understanding its structure and properties.

Recently, we developed a hydrothermal method for manufacturing almost impurity-free flakes of 10-200 nm in lateral size and 10-20 nm thick of synthetic valleriite [29] and tochilinite [30], including doped with Al, Li, 3d metals, and examined some of their main characteristics using XRD, TEM, EDS, X-ray photoelectron spectroscopy (XPS), reflection electron energy loss spectroscopy, Mössbauer, Raman and UV-vis-NIR spectroscopies, together with magnetization, impedance, zeta potential and other measurements [31-32]. The hydroxide and sulfide layers are stacked due to their opposite electric charges but not van der Waals forces; it was found that Al cations entered hydroxide layers decreasing the amount of Fe in the layers ranged from 10 to 45% of total iron, and surprisingly increasing their negative charge whereas the effect of Li is inverse [31]. The valleriite-type materials were highlighted as a new family of 2D materials with promising but still almost unexplored physical and chemical properties.

Information about stability and reactions of valleriites at enhanced temperatures are required for many potential applications; in addition, that is necessary for understanding the fundamentals of chemistry of 2D layered materials, and is of practical importance for mineral processing and metallurgy. Few previous studies mentioned temperature effects in the formation and stability of valleriite [32-33] have been performed with the samples contained less than 50% of the target substance. The goal of the current research was to elucidate stability ranges and reactions of valleriite, including doped with Al and Li, at temperatures up to 1000 ºC by thermogravimetry (TG, DTG) and differential scanning calorimetry (DSC) under inert and oxidizing conditions. We have also employed XPS, XRD, SEM, and TEM to characterize the initial materials and the final products. The results were compared with the DTA data available in the literature for bulk brucite, chalcopyrite, and layered double hydroxides to gain insights into mechanisms behind specific behavior and mutual influence of the 2D sulfide and hydroxide layers.

2. Materials and methods

2.1. Materials and synthetic procedures

Analytical grade commercial iron (II) sulfate $FeSO_4\cdot 7H_2O$, copper sulfate $CuSO_4\cdot 5H_2O$, sodium sulfide $Na_2S\cdot 9H_2O$, magnesium sulfate $MgSO_4\cdot 7H_2O$, aluminum sulfate $Al_2(SO_4)_3\cdot 18H_2O$, lithium hydroxide ($LiOH\cdot H_2O$) and aqueous ammonia were used without further purification in synthesis of valleriites. Millipore Milli-Q grade deionized water (specific resistivity > 18 M) was utilized to prepare precursor solutions and to wash the reaction products. The procedures and installation for preparation of valleriite flakes as well as characteristics of the products were described detail elsewhere [29]. In brief, a typical procedure, pre-determined quantities of Fe and Cu sulfates were transferred to a small water volume and a freshly prepared 20% solution of Na_2S was slowly added under agitation, which gave rise to metal sulfide black

precipitates. Magnesium hydroxide or its mixture with aluminum or/and hydroxide were prepared by adding 25% aqueous ammonia to solutions of Mg and Al sulfates (Li hydroxide). The dispersion was transferred to the glass with Fe and Cu sulfides, pH was adjusted to 10–11 with aqueous ammonia, and the mixture was loaded into an in-home made stainless steel autoclave with Teflon liner. The vessel was purged with Ar and sealed and then heated to 160 °C using an air thermostat during about 50 h. the autoclave was cooled in air, and the solid products were separated and washed with water in 4–5 centrifugation - redispersion cycles. The residue was dried in air at room temperature before examination. The initial atomic proportions of precursors and designations of the samples employed in this study are summarized in Table 1.

Table 1. Atomic proportions of precursors used in hydrothermal synthesis of valleriite samples and their designations

Sample	Atomic proportions of precursors					
	Fe	Cu	Mg	Al	S	Li
a	2	2	2	-	15	-
b	2	2	2	0.5	15	0.5
c	2	2	2	0.5	15	-
d	2	2	2	-	15	0.5

2.2 Characterization

The thermogravimetric (TG/DTG) measurement and differential scanning calorimetric (DSC) analyses were performed in a temperature range from 20 to 1000 ºC using a STA449 F1 Jupiter instrument (Netzsch, Germany) at a heating rate of 10 ºC/min in inert (Ar) and oxidative (N_2 80 vol.%, O_2 20 vol.%) gas flow with a rate of 50 mL/min.

X-ray powder diffraction patterns were acquired from air-dried synthetic valleriite and the reaction products (heated mainly to 1000 ºC during the DTA experiments and cooled to room temperature) using a PANalytical X'Pert Pro diffractometer with Cu Kα radiation. Rietveld refinement was performed using TOPAS3 software, with information about reference structures borrowed from Crystallography Open Database (http://www.crystallography.net/cod/).

SEM images were acquired with a TM4000 microscope (Hitachi, Japan) operated at the accelerating voltage of 15 kV equipped with microprobe system Quantax 70 (Bruker, Germany) that was utilized for EDX analyses of elemental composition.

X-ray photoelectron spectra were measured with a SPECS instrument (SPECS, Germany) equipped with a PHOIBOS 150 MCD-9 analyzer operated at the pass energy of 20 eV for survey spectra and 10 eV for high-resolution spectra. Monochromatic Al Kα irradiation (1486.7 eV) was used for excitation. The high-resolution spectra were fitted with Gaussian–Lorentzian peak profiles after subtraction of the Shirley-type background; the Fe 2p spectra were fitted with two sets of multiplet lines [34] for Fe^{3+} cations bonded to hydroxide and sulfide anions. More details on the methods and results for analogous valleriite samples can be found in Ref. [29].

3. Results and Discussion

3.1 Structure, morphology and composition of valleriites

Figure 1 shows a sketch of valleriite structure (Fig. 1A) [31] and typical TEM images (Fig. 1B, C) obtained for the sample *a* synthesized using atomic precursor proportions of Fe 2 Cu 2 Mg 2 S 15. Valleriite forms nanoflakes of ~100-200 nm in the lateral size and 10-20 nm thick, with

the interlayer distance being of ~1.11 nm, that is, the flakes are constructed by roughly a dozen of stacked sulfide and hydroxide monolayers. The XRD patterns collected from the samples *a-d* (Fig. 1D) exhibit the reflections of valleriite, which are in a good agreement with the literature data [15-17] and insignificantly alter due to addition of Al and Li dopants [31]. For all the samples, valleriite is the only crystalline phase, although very minor impurities of brucite were found in some cases (Fig. 1F). This corroborates also with chemical compositions of the samples (see Table 2 below). XPS spectra (Fig. 1E, F, see also ESI) allow to elucidate the chemical state of elements in the valleriites. In particular, the Fe 2p spectra (Fig. 1F) of as-synthesized materials can be fitted with two sets of lines corresponding to Fe^{3+}-OH centers in hydroxide layers (first peak at 711.7 eV), and Fe^{3+}-S species in sulfide layers (first peak at 707.9 eV). The contribution of Fe^{3+}-OH species was bigger for samples, in which Mg^{2+}-ions were partially substituted with Li^{+}-ions, and lesser when Mg^{2+}-ions were partially substituted with Al. In general, the XPS data coincide with those measured and discussed in detail for similar valleriite specimens previously [29, 31, 32].

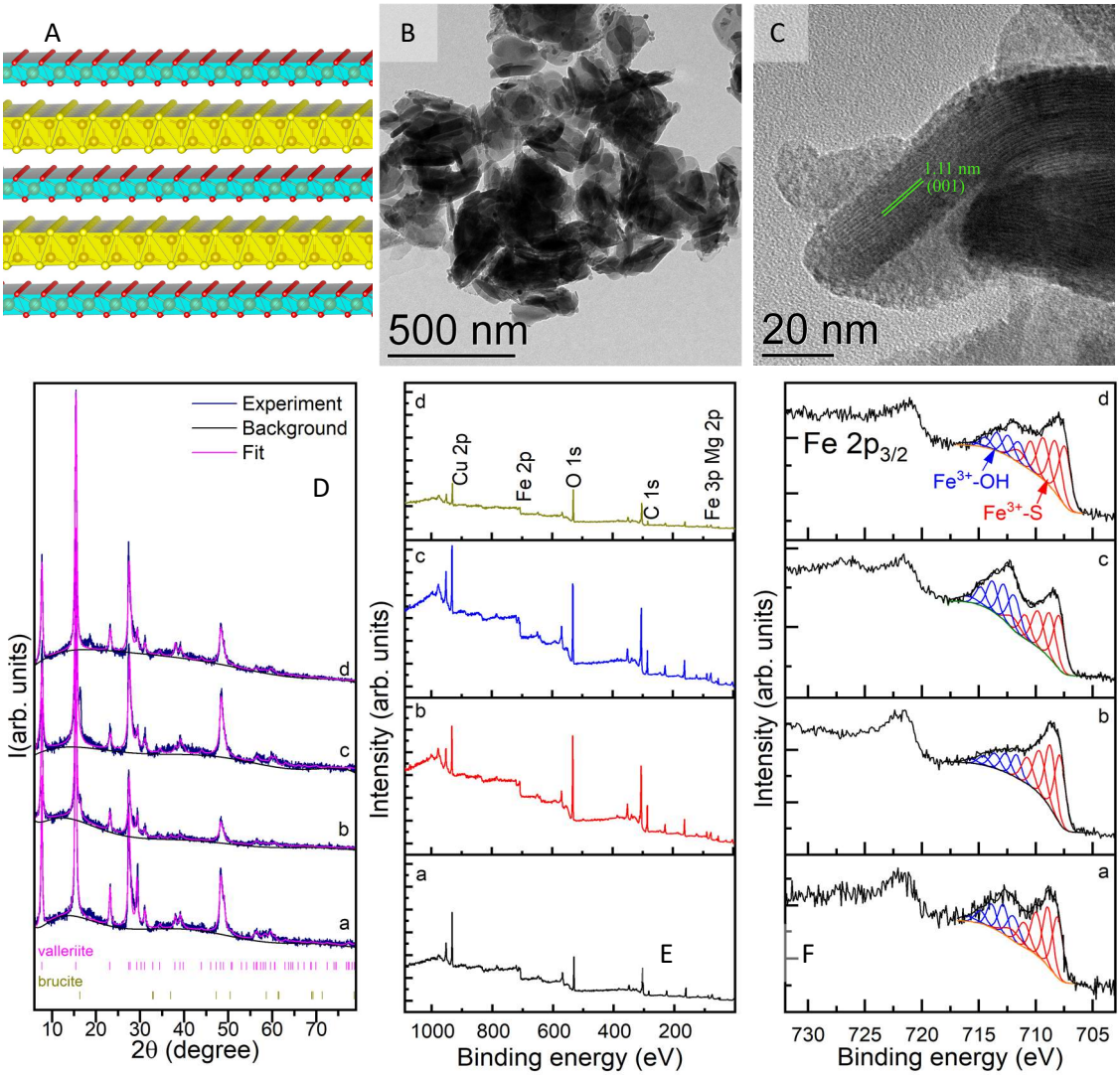

Figure 1. A schematic representation of valleriite structure (A) composing of alternating brucite-like and $CuFeS_2$-like layers, TEM micrographs (B, C) of sample *a*. (D) XRD patterns, (E) wide scan and (F) Fe 2p spectra of the samples a-d.

3.2 Thermal behavior

3.2.1. Inert atmosphere

Figure 2 shows the results of thermogravimetric analysis (TGA) and differential scanning calorimetry (DSC) acquired for the valleriite samples synthesized without and with adding of Al or Li salts or both (Table 1) upon heating in Ar. A slow mass decrease (~2-3%) with small endothermic effects at the temperatures below 300 ºC (Fig. 1A-D) can be accounted for the loss of moisture and weakly bonded water that is typical for metal hydroxides [10-12, 35-43]. The loss of about 12 % mass takes place in the range from ~350 to 600 ºC in two or three stages, with the main endothermic DSC peak arisen at 413 ºC. Interestingly, it shifts at 498 ºC for the samples containing Al (and Al+Li) and hence diminished amount of Fe in the hydroxide layers (ESI, see also [31]). The second decomposition stage causes the weight decrease that is smaller, especially for the Al-doped samples, and is accompanied by slight endothermic effects at 500-600 ºC. The effect of addition of Li is much less expressed than that Al in all the stages. Similar processes reported for bulk brucite have been attributed to the formation of defect magnesium oxide keeping the brucite structure and containing residual OH groups, and then MgO with face centered cubic unit cell (periclase) [41]. In particular, Nahdi et al. [35] have reported the temperature of the major endothermic peak of 415 ºC and smaller one at 510 ºC, in well agreement with the current data upon heating in air. The reactions of brucite depend on the material composition and impurities, morphology and gas environment [36-40], so the comparison with valleriite is not straightforward, especially due to assembling with metal sulfide part.

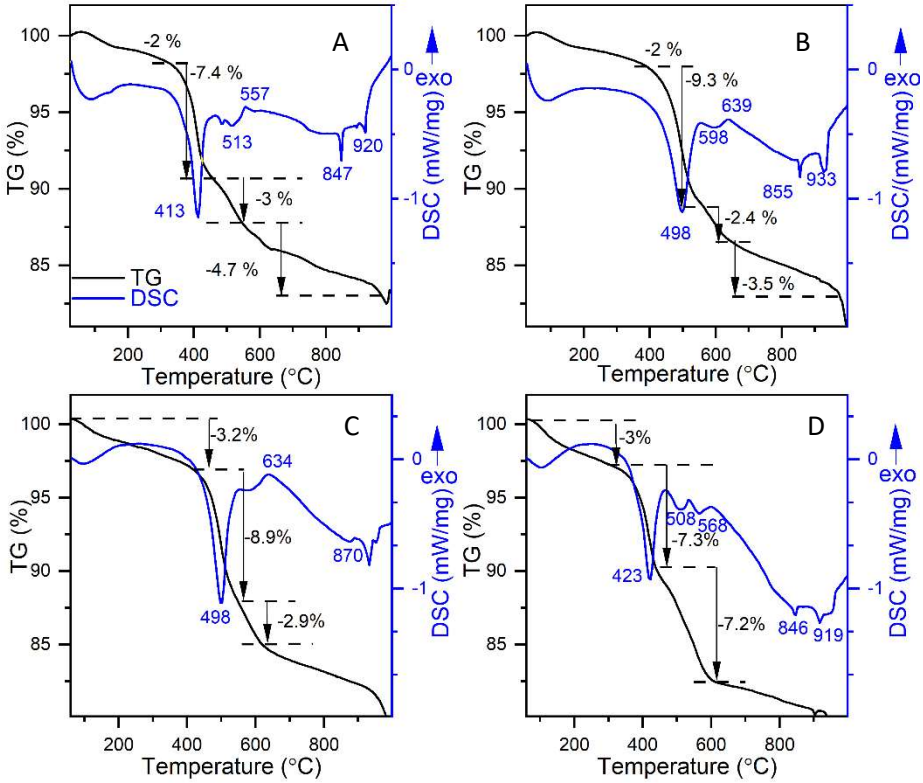

Figure 2. TGA and DSC profiles acquired in Ar media for synthetic valleriite samples prepared using no additives (A), or using both Al and Li (B), only Al (C) and only Li (D) as modifiers.

Solid-state transformations of bulk Cu-Fe sulfides involving the tetragonal-cubic transition in chalcopyrite in the vicinity of 560 °C [44] and formation of intermediate solid solutions above approximately 550 °C followed by melting and solid-liquid reactions in the Fe-Cu-S system at higher temperatures [45-48] yield bornite Cu_5FeS_4, chalcopyrite $CuFeS_2$, and troilite FeS [45, 46]. The share of bornite is largest because of its higher temperature stability than that of chalcopyrite [47]. The melting points have been reported in the range 840-880 °C for monophase chalcopyrite and bornite, and 1100 °C for FeS, while a sulfide liquid emerges in the Cu-Fe-S system below 800 °C. For valleriite, the same processes at similar temperatures probably manifest themselves by some decrease of the weight due to evaporation of sulfur (about 3 %) and wide endothermic band overlapped with small narrow peaks, e.g. at 847 and 920 °C.

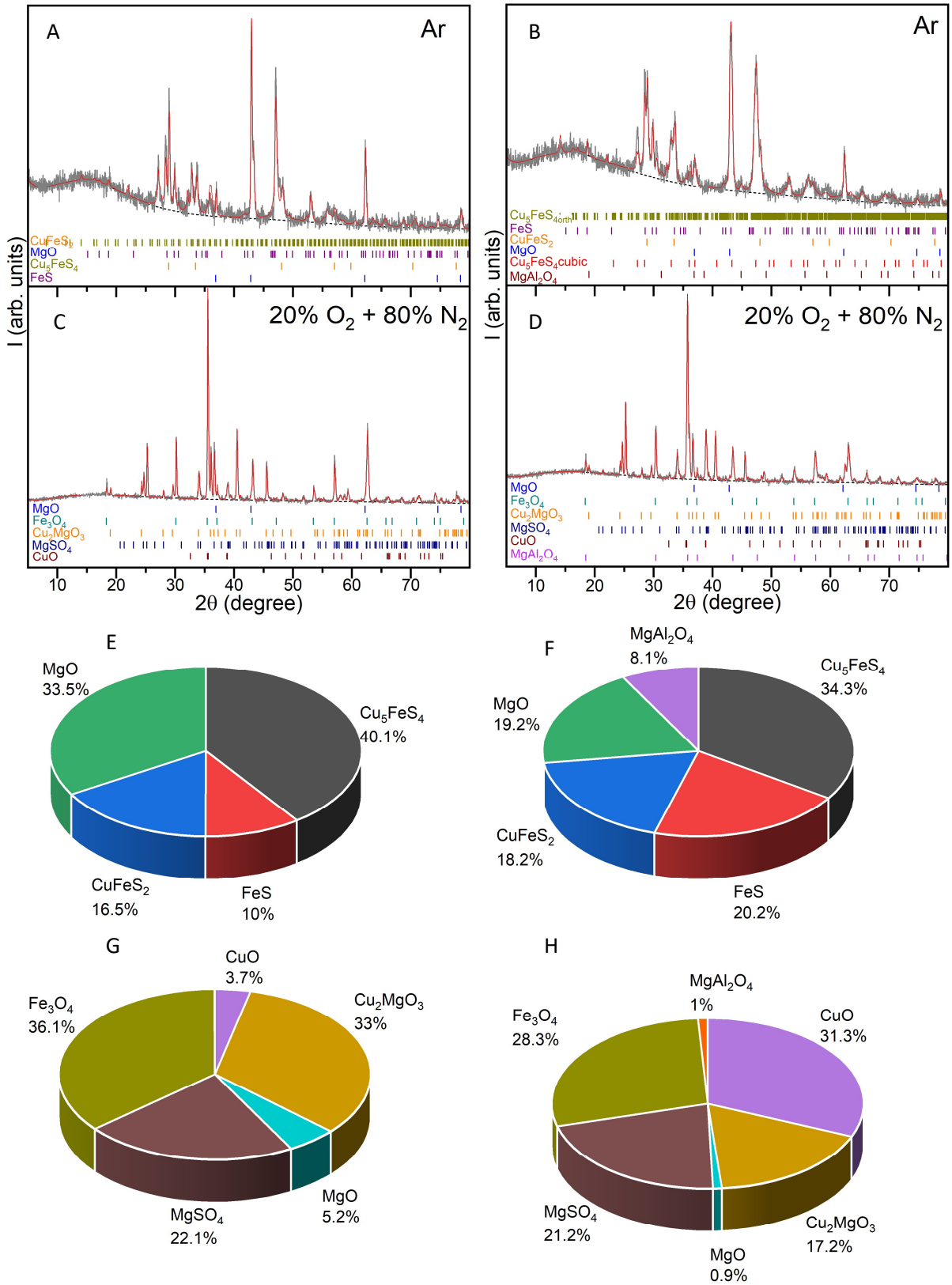

Figure 3. X-ray diffraction patterns of synthetic valleriite non-substituted (A, C) and substituted with both Al and Li (B, D) after the heating to 1000 °C. All the phase fractions are given in wt. %. A, B – in Ar fow, C, D – in 80% N_2 + 20% O_2 gas mixture. E - H –phase speciation corresponding to XRD patterns A – D.

This interpretation is supported by the chemical and phase compositions of the products of heating (Fig. 3). The EDX analysis (Table 2) shows that the content of sulfur reduces but remains

substantial, with the atomic Cu/S ratio changed from 1:2 to 1:1.5. The XRD examination revealed periclase MgO in the case of undoped sample, and MgO plus $MgAl_2O_4$ for the samples synthesized with Al and Li, and Cu_5FeS_4, $CuFeS_2$ and FeS in both cases, although in somewhat different proportions. The share of bornite is largest owing to its higher temperature stability than that of chalcopyrite [47]. The micrometer-scale melt droplets can be seen in SEM micrographs of the cooled products (ESI). Therefore, valleriite heating in Ar atmosphere at the temperatures >500 °C can be principally explained by the behavior of its sulfidic components and is similar to that of the bulk sulfides. This implies that the structure of valleriite disappeared after the decomposition of 2D brucite-like layers and the formation of quasi-bulk MgO species (Fig. 3), promoting the coalescence of sulfidic sheets.

Table 2. Chemical composition of valleriites (at.%) determined using EDS synthesized using atomic proportions of reagents Fe 2 Cu 2 Mg 2 S 15, (a) without heating, (b) after heating to 1000 °C in Ar media and (c) after heating to 1000 °C in 80% N_2 + 20% O_2 mixture*.

Sample	Elements				
	Fe	Cu	Mg	O	S
a	22.0	14.4	21.6	12.0	30.0
b	19.9	13.5	32.5	13.8	20.3
c	9.4	28.2	21.6	26.6	14.2

*Averaging was performed over a series of elemental maps, not over the spots.

3.2.1. Oxidizing atmosphere

Fig. 4 shows TG and DSC curves for heating of valleriites in oxygen-containing gas flow (20 vol.% O_2). Aside from the initial loss of water, there are exothermic reactions at 345 °C with increasing the sample mass by about 4%, the main feature at 495 °C corresponding to the mass growth on the order of 20%, and a smaller mass increase (about 5%) with lesser energy effects in the range of 550 – 750 °C suggest oxidation of sulfide part of valleriite. At higher temperatures, the mass decreases by about 25% in weakly endothermic reactions. Oxidation of Cu-Fe sulfides, particularly chalcopyrite $CuFeS_2$, has been intensively studied for metallurgical roasting [49-51] but the reaction mechanisms are not completely understood yet. Oxidation usually proceeds in several stages, depending on the particle size, heating rate and so accessibility of the metal sulfides to oxygen [52]. Taking in mind the thermal behavior of chalcopyrite [44-46, 52] and valleriite in inert media, we suggest that partial decomposition of the sulfide layers to copper and iron sulfides, preferentially bornite Cu_5FeS_4, and iron oxides result in the exothermic maxima at 300-350 °C. The increase in the sample mass indicates that oxidized sulfur remains in the samples either as elemental sulfur or, more likely, as metal sulfates due to entrapping and oxidation of SO_2, possibly in both layers. The main oxidation peak at the temperatures above 400 °C for chalcopyrite is due to oxidation of the main portion of metal sulfides yielding $CuSO_4$, $CuO{\cdot}CuSO_4$, Fe sulfate and oxide (α-Fe_2O_3) [49-52], and this could the case for valleriite too, with a minor mass growth attributable to oxidation of residual copper sulfides, e.g. Cu_2S. The process appears to occur simultaneously with the decay of magnesium-based hydroxides above 500 °C, and copper and iron sulfates losing SO_2 at the temperatures higher than 600 °C [49, 52].

XRD, EDX and XPS examination (Fig. 3, Table 2 and Fig. S3, correspondingly) found out the final products different from those for oxidation of chalcopyrite and for valleriite heated in inert atmosphere. The yields of CuO (tenorite) and MgO were surprisingly low, and Cu-Fe-O compounds were absent, whereas substantial quantities of $MgSO_4$ and Cu_2MgO_3 formed, suggesting a sort of mixing the layers. It is also noteworthy that magnetite Fe_3O_4 instead of more often hematite [52] was detected, and proportions of the products varied for the samples with and without Al and Li.

In contrast to Ar atmosphere, the samples modified with Al or Li or both show the TG and DSC peaks shifted to lower temperatures, with the main peak temperature (initially 495 ºC) dismissed by about 60 °C and the preliminary one decreased by about 30 ºC (10 ºC for doping with Li). Also, an increase in the mass growth was observed in the low-temperature stage. The findings cannot be plainly explained by a disorder induced by foreign cations in the hydroxide sheets, facilitating access of oxygen to and removal of sulfur species from metal sulfide layers upon oxidation, since this seemingly contradicts the behavior in inert media; it also implies that the content of Fe in the hydroxide layer is of negligible importance.

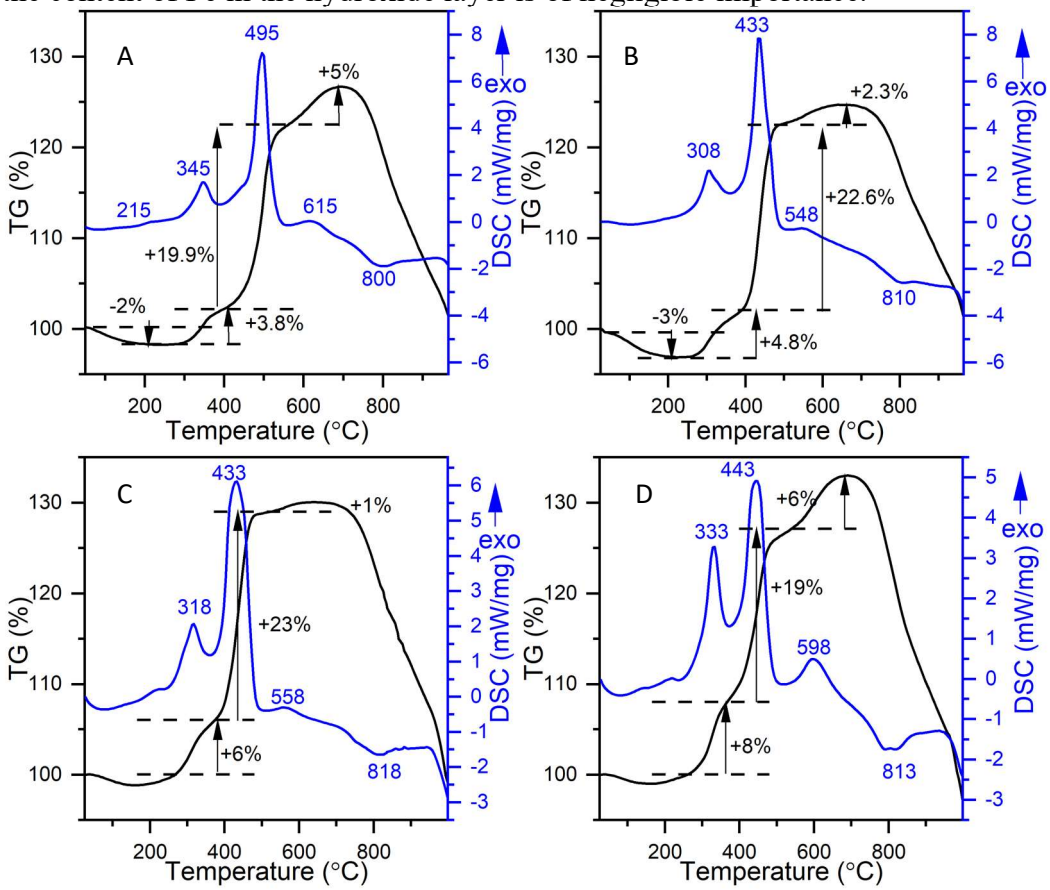

Figure 4. TGA and DSC profiles for synthetic valleriite samples prepared using no additives (A), or using both Al and Li+ (B), only Al (C) and only Li (D) as substitutes for Mg^{2+} in hydroxide layers. All the curves were acquired in 20% O_2 + 80% N_2 mixture.

4. Discussion

We have demonstrated that the thermal behavior of valleriite in non-oxidative media resembles that of brucite [35-43] and the oxidative reactions are similar to oxidation of chalcopyrite [49-52]. At the same time, the differences allow elucidating some specific characteristics of two-dimensional layered structures, including the effect of doping with Al^{3+} and Li^{+} cations replacing a share of Mg^{2+} cations and controlling the amount of Fe^{3+} centers in hydroxide layers. Under all the conditions, the samples lost adsorbed water and then H_2O molecules due to limited dehydration of brucite-based sheets (up to about 3% of total mass), keeping the structure of magnesium hydroxide at the temperatures less than 250-300 °C. Moreover, the crystalline lattice of brucite is believed to retain in defective magnesium oxide formed at temperatures as high as ~500 °C [35, 41]. Further heating in non-oxidative atmosphere can be principally explained by the behavior of the sulfidic components which is similar to that of the bulk sulfides, including the formation of bornite, chalcopyrite and troilite via solid-liquid (sulfidic melt) reactions. This means that the layered structure of valleriite disappeared after decomposition and transformation of 2D brucite-like layers, which prevented the coalescence of sulfidic sheets, to quasi-bulk MgO species (Fig. 4). It is interesting that no discernible chemical interactions between sulfide and hydroxide entities

were observed in the inert media (at very high temperatures, this is due to poor wetting of Mg oxides by melted Cu-Fe sulfides, at least in part).

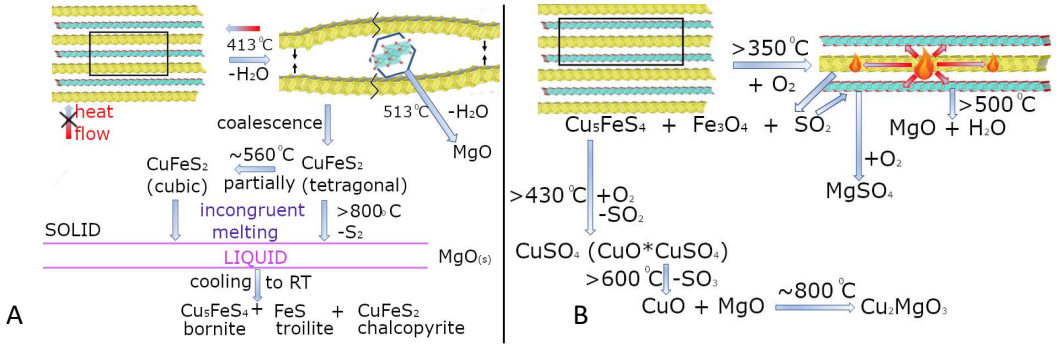

Figure 5. Schematic presentation of thermal decomposition reactions occurring in inert (A) and oxidizing (B) media.

The decomposition of valleriite in oxygen-containing gas is exothermic and proceeds with increase of the sample mass till 600-800 °C due to oxidation of Cu-Fe-S layers and the formation of metal sulfates; sulfates of Cu and Fe start decomposing above 600 °C. The big amounts of $MgSO_4$, which is more energy favorable than sulfates of other metals, and only minor MgO in the final products suggest that SO_2/SO_3 reacted with Mg hydroxide rather than with inert MgO, that is, in rather early reaction stages. The appearance of magnesium sulfate should compromise the brucite-type layers much stronger than cations replacing Mg in its lattice. The formation of Cu_2MgO_3 instead of $CuFeO_4$ is also indicative of mixing the layer components. Therefore, oxidation of Cu-Fe sulfides promotes degradation of magnesium hydroxide layers, and, in turn, that accelerates the oxidation of metal sulfides, and their blending with oxide species. Probably, the products still limit access of oxygen so magnetite but not hematite arises upon oxidation.

It must be underlined that the thermal reactivity of valleriite, particularly $Mg(OH)_2$-based sheets, in inert medium is comparable, or even lower, despite the 2D structure, than that of their bulk brucite and chalcopyrite counterparts. Another intriguing feature is the higher stability of hydroxide layers doped with Al and, much less significant, Li, in non-oxidative conditions, while Al and, slightly less, Li effectively promote oxidation of valleriites. These phenomena can be tentatively explained as follows. Vaziri et al. [53] have recently discovered ultrahigh thermal resistance across the heterostructures constructed by of stacked monolayers of graphene, MoS_2 and WSe_2. The authors concluded that the thermal isolation of the layers originates from the mismatch in mass and phonon density of states between the 2D layers. We hypothesize that this is the case for incommensurate quasi-atomic (Cu, Fe) sulfide and Mg hydroxide layers in valleriite too. The thermal isolation should retard the endothermic reactions requiring influx of energy, i.e., transformations of the hydroxide and, in less extent, sulfide sheets in Ar atmosphere. On contrast, the energy released in exothermic oxidation of metal sulfides is accumulated within the layers, accelerating the reactions. As already mentioned, Al decreases and Li somewhat increases the concentration of Fe in the hydroxide layers [29] (see also fig. 1F). The presence of comparable numbers of Fe cations with the same atomic mass in both layers should improve the phonon and heat transfer between them. As a result, the addition of Al decreasing the content of Fe in the hydroxide part increases the thermal resistance across the valleriite layers and slows down the endothermic reactions (Fig. 2), and the opposite is true for exothermic reactions of sulfide oxidation (Fig. 5). Certainly, the mechanisms behind these phenomena still need to be understood in detail.

The results of this research shed light onto the chemical reactivity of 2D materials of the valleriite family and pave the way for tuning their characteristics, including in new applications, where thermal behavior is important.

5. Conclusions

We examined thermal stability and reactivity of nanoflakes of synthetic valleriite samples in oxidative and inert gas media using TG/DTG and DSC methods. The dehydroxylation of the hydroxide layers yielding finally MgO in Ar atmosphere proceeds with the loss of about 12% of mass in several stages in the range from ~350 to 600 ºC, with the major endothermic DSC peak at 413°C. The peaks shift to 498 ºC for the valleriites containing Al and Al+Li dopants and so reduced amount of Fe in the hydroxide layers. Sulfide sheets start to decompose below 500 °C and to melt nearby 800 °C, with evaporation some sulfur and formation of bornite, chalcopyrite and troilite as the final products. In the oxidative atmosphere, the exothermic maxima accompyning the mass increase at 345 and 495 °C correspond to a partial and principal oxidation of Cu-Fe sulfide layers, respectively. The samples modified with Al or Li or both show the peaks shifted to lower temperatures by 10-30 ºC and about 60 °C (the major one). Sulfur oxides are entrapped by magnesium hydroxide layers forming $MgSO_4$; this probably compromises the layer structure, facilitating influx of oxygen and oxidation of the sulfide sheets. The final products are composed, in addition to magnesium sulfate, of rather small amount of MgO, Cu_2MgO_3, Fe_3O_4 and $MgFe_2O_4$. We rationalized the results in terms of the mutual influence of the 2D hydroxide and sulfide layers on the transport of reagents (oxygen) and reaction products (e.g., sulfur oxides) and, following to ref. [-], by high thermal resistance across the stacked incommensurate sheets containing atoms with essentially different masses. Particularly, this impeded the endothermic reactions in Ar flow and accelerated the exothermic oxidation of Fe and Cu sulfides. The high concentrations of Fe atoms in the hydroxide sheets are expected to promote the phonon and heat transfer between the layers. These phenomena entail the surprising stability of valleriite in comparison with bulk brucite and chalcopyrite, at least in inert media. The results also indicate how the thermal effects can be tailored by modifying the composition of valleriite.

Supporting Information

Additional XRD, XPS, SEM images, corresponding elemental maps and EDS analysis results.

Acknowledgements

This research was financially supported by the Russian Science Foundation, project 22-13-00321. Facilities of the Krasnoyarsk Regional Center of Research Equipment of Federal Research Center «Krasnoyarsk Science Center SB RAS» were employed in the work.

Conflicts of interest

There are no conflicts to declare.

References

1. He, Z.; Que, W. Molybdenum disulfide nanomaterials: structures, properties, synthesis and recent progress on hydrogen evolution reaction. *Appl. Mater. Today* **2016**, *3*, 23-56.
2. Du, Z.; Yang, S.; Li, S.; Lou, J.; Zhang, S.; Wang, S.; Li, B.; Gong, Y.; Song, L.; Zou, X.; Ajayan, P. M. Conversion of non-van der Waals solids to 2D transition-metal chalcogenides. *Nature* **2020**, *577*, 492-496.
3. Monga, D.; Sharma, S.; Shetti, N.P.; Basu, S.; Reddy, K.R.; Aminabhavi, T.M. Advances in transition metal dichalcogenide-based two-dimensional nanomaterials. *Mater. Today Chem.* **2021**, *19*, 100399.
4. Gogotsi, Y.; Anasori, B. The Rise of MXenes. *ACS Nano* **2019**, *13*, 8491–8494.
5. Cheng, Y.-W.; Dai, J.-H.; Zhang, Y.-M.; Song, Y. Two-dimensional, ordered, double transition metal carbides (MXenes): a new family of promising catalysts for the hydrogen evolution reaction. *J. Phys. Chem. C* **2018**, *122*, 28113-28122.

6. Verger, L.; Natu, V.; Carey, M.; Barsoum, M.W. MXenes: an introduction of their synthesis, select properties, and applications. *Trends Chem.* **2019**, *1*, 656-669.
7. Kim, H.; Alshareef, H. N. MXetronics: MXene-enabled electronic and photonic devices, *ACS Materials Lett.* **2020**, *2*, 55–70.
8. Naclerio, A.E.; Kidambi, P.R. A Review of scalable hexagonal boron nitride (h-BN) synthesis for present and future applications. *Adv. Mater.* **2023**, *35*, 2207374.
9. Eichler, J.; Lesniak, C. Boron nitride (BN) and BN composites for high-temperature applications. *Journal of the European Ceramic Society* **2008**, *28*, 1105-1109.
10. Layered Double Hydroxides. Volume Eds X. Duan, D.G. Springer-Verlag, Berlin, 2006. 234 p.
11. Layered Double Hydroxide Polymer Nanocomposites. Eds. S. Thomas, S. Daniel. Elsevier, 2020. 858 p.
12. Karim, A. V.; Hassani, A.; Eghbali, P.; Nidheesh, P. V. Nanostructured modified layered double hydroxides (LDHs)-based catalysts: A review on synthesis, characterization, and applications in water remediation by advanced oxidation processes. *Current Opinion in Solid State and Materials Science* **2022**, *26*, 100965.
13. Xu, M.; Lian, T.; Shi, M.; Chen H. Graphene-like two-dimensional materials. *Chem. Rev.* **2013**, *113*, 3766–3798.
14. Tiwari, S.K.; Sahoo, S.; Wang, N.; Huczko A. Graphene research and their outputs: status and prospect. *J. Sci.: Adv. Mater. Devices* **2020**, *5*, 10-29.
15. Evans, H.T. Jr.; Allman R. The crystal structure and crystal chemistry of valleriite. *Z. für Kristallogr.* **1968**, *1968127*, 73-93.
16. Cabri, L.J. A new copper-iron sulfide. *Econ. Geol.* **1967**, 62, 910-925.
17. Organova, N.I. Crystallochemistry of modulated and incommensurate structures in minerals. *Int. Geol. Rev.* **1986**, *28*, 802-814.
18. Waanders, F.B.; Pollak, H. Mössbauer spectroscopy to characterize iron sulphides. *South Afr. J. Sci.* **1999**, *95*, 387-390.
19. Mücke, A. Review on mackinawite and valleriite: Formulae, localities, associations and intergrowths of the minerals, mode of formation and optical features in reflected light. *J. Earth Sci. Clim. Change* **2017**, *8*, 1000419.
20. Hughes, A.E.; Kakos, G.A.; Turney, T.W.; Williams, T.B. Synthesis and structure of valleriite, a layered metal hydroxide/sulfide composite. *J. Solid State Chem.* **1993**, *104*, 422-436.
21. Pachmayr, U.; Johrendt, D. [(Li 0.8 Fe 0.2) OH] FeS and the ferromagnetic superconductors [(Li 0.8 Fe 0.2) OH] Fe (S 1− x Se x)(0< x≤ 1). *Chemical Communications* **2015**, *51*, 4689-4692.
22. Dong, X.; Jin, K.; Yuan, D.; Zhou, H.; Yuan, J.; Huang, Y. et al. (Li 0.84 Fe 0.16) OHFe 0.98 Se superconductor: Ion-exchange synthesis of large single-crystal and highly two-dimensional electron properties. *Phys. Rev. B* **2015**, *92*, 064515.
23. Hu, G.; Shi, M.; Wang, W.; Zhu, C.; Sun, Z.; Cui, J. et al. (). Superconductivity at 40 K in lithiation-processed [(Fe, Al)(OH) 2][FeSe] 1.2 with a layered structure. *Inorg. Chem.* **2021**, *60*, 3902-3908.
24. Pekov, I. V.; Sereda, E. V.; Polekhovsky, Y. S.; Britvin, S. N.; Chukanov, N. V.; Yapaskurt, V. O.; Bryzgalov, I. A. (). Ferrotochilinite, 6FeS· 5Fe (OH) 2, a new mineral from the Oktyabr'sky deposit, Noril'sk district, Siberia, Russia. *Geol. Ore Deposits* **2013**, *55*, 567-574.
25. Pekov, I. V.; Sereda, E. V.; Yapaskurt, V. O.; Polekhovsky, Y. S.; Britvin, S. N.; Chukanov, N. V. Ferrovalleriite, 2 (Fe, Cu) S· 1.5 Fe (OH) 2: validation as a mineral species and new data. *Geol. Ore Deposits* **2013**, *55*, 637-647.
26. D.C. Harris; L.J. Cabri; Stewart J.M. A "valleriite-type" mineral from Noril'sk, Western Siberia. *Am. Mineral.* **1970**, *55*, 2110-2114.

27. Genkin, A. D.; Distler, V. V.; Gladyshev, G. D. Sul'fidnye Medno-Nikelevye Rudy Noril'skikh Mestorozhdenii (Sulphidic Copper-Nickel Ores of Noril'sk Deposits); Nauka: Moscow, 1981; p 234, (in Russian).
28. Dodin, D. A. Metallogeniya Taimyro-Noril'skogo regiona (Metallogeny of Taimyr-Noril'sk region); Nauka: St.-Petersburg, 2002; p 374. (in Russian).
29. Mikhlin, Y. L.; Borisov. R. V.; Vorobyev, S. A.; Tomashevich, Y. V.; Romanchenko, A. S.; Likhatski, M. N.; Karacharov, A.A.; Bayukov, O.A.; Knyazev, Y.V.; Velikanov, D.A.; Zharkov, S.M.; Krylov, A.S.; Krylova, S.N.; Nemtsev, I. V. Synthesis and characterization of nanoscale composite particles formed by 2D layers of Cu–Fe sulfide and Mg-based hydroxide. *J. Mater. Chem. A.* **2022**, *10*, 9621-9634.
30. Mikhlin, Yu.L.; Borisov, R.V.; Likhatski, M.N.; Bayukov, O.D.; Knyazev, Yu.V.; Zharkov, S.M.; Vorobyev, S.A. et al. Facile synthesis and selected characteristics of two-dimensional material composed of iron sulfide and magnesium-based hydroxide layers (tochilinite). ChemRxiv. Cambridge: Cambridge Open Engage **2022** This content is a preprint and has not been peer-reviewed.
31. Mikhlin, Yu. L.; Likhatski, M. N.; Bayukov, O. A.; Knyazev, Yu.V.; Velikanov, D. A., Tomashevich, Ye. V.; Romanchenko, A.S.; Vorobyev, S.A.; Volochaev, M.V.; Zharkov, S.M.; Meira, D. M. Valleriite, a Natural Two-Dimensional Composite: X-ray Absorption, Photoelectron, and Mossbauer Spectroscopy, and Magnetic Characterization. *ACS Omega*. **2021**, *6*, 7533-7543.
32. Mikhlin, Yu.L.; Likhatski, M.N.; Romanchenko, A.S.; Vorobyev, S.A; Tomashevich, Ye.V.; Fetisova, O.Yu. et. al Valleriite-containing ore from Kingash deposit (Siberia, Russia): Mössbauer and X-ray photoelectron spectroscopy characterization, thermal and interfacial properties. *J. Sib. Fed. Uni.* **2022**, *15*, 303-317.
33. Li, R.; Cui, L. Investigations on valleriite from Western China: crystal chemistry and separation properties. *Int. J. Miner. Process*. **1994**, *41*, 271-283.
34. A.P. Grosvenor, B.A. Kobe, M.C. Biesinger, N.S. McIntyre, Investigation of multiplet splitting of Fe 2p XPS spectra and bonding in iron compounds. *Surf. Interface Anal.* **2004**, *36*, 1564-1574.
35. Nahdi, K.; Rouquerol, F.; Ayadi, M.T. $Mg(OH)_2$ dehydroxylation: A kinetic study by controlled rate thermal analysis (CRTA). *Solid State Sci.* **2009**, *11*, 1028–1034.
36. Rajamathi, M.; Nataraja, G. D.; Ananthamurthyb, S.; Kamath, P.V. Reversible thermal behavior of the layered double hydroxide of Mg with Al: mechanistic studies. *J. Mater. Chem.* **2000**, *10*, 2754-2757.
37. Valcheva-Traikova, M.L.; Davidova, N.P.; Weiss A.H. Thermal decomposition of Mg, Al-hydrotalcite material. *J. Mater. Sci.* **1993**, 28, 2157-2162.
38. Aramendía, M.A.; Avilés, Y.; Borau, V.; Luque, J.M.; Marinas, J.M.; Ruiz, J.R.; Urbano, F.J. Thermal decomposition of Mg/Al and Mg/Ga layered-double hydroxides: a spectroscopic study. *J. Mater. Chem.* **1999**, *9*, 1603-1607.
39. Shabanian, M.; Basaki, N.; Khonakdar, H. A.; Jafari, S. H.; Hedayati, K.; Wagenknecht, U. Novel nanocomposites consisting of a semi-crystalline polyamide and Mg–Al LDH: Morphology, thermal properties and flame retardancy. *Appl. Clay Sci.* **2014**, *90*, 101-108.
40. Kanezaki, E. (). Thermal behavior of the hydrotalcite-like layered structure of Mg and Al-layered double hydroxides with interlayer carbonate by means of in situ powder HTXRD and DTA/TG. *Solid State Ionics* **1998**, *106*, 279-284.
41. Kondo, A.; Kurosawa, R.; Ryu, J.; Matsuoka, M.; Takeuchi, M. Investigation on the Mechanisms of $Mg(OH)_2$ Dehydration and MgO Hydration by Near-Infrared Spectroscopy. *J. Phys. Chem. C* **2021**, *125*, 10937−10947.
42. Kurosawa, R.; Takeuchi, M.; Ryu J. Comparison of the Effect of Coaddition of Li Compounds and Addition of a Single Li Compound on Reactivity and Structure of Magnesium Hydroxide. *ACS Omega* **2019**, *4*, 17752−17761.

43. Shkatulov, A.; Krieger, T.; Zaikovskii, V.; Chesalov, Y.; Aristov, Y. Doping magnesium hydroxide with sodium nitrate: A new approach to tune the dehydration reactivity of heat-storage materials. *ACS Appl. Mater. Interfaces* **2014**, *6*, 19966-19977.
44. J. E. Dutrizac. Reactions of cubanite and chalcopyrite. *Can. Miner.* **1976**, *14*, 172-181.
45. Shima, H. Studies on chalcopyrite (I) Transformation and dissociation of chalcopyrite heated in argon atmosphere. *The Journal of the Japanese Association of Mineralogists, Petrologists and Economic Geologists* **1962**, *47*, 123-133.
46. Baláž, P.; Tkáčová, K.; Avvakumov, E. G. The effect of mechanical activation on the thermal decomposition of chalcopyrite. *J. Therm. Anal.* **1989**, *35*, 1325-1330.
47. Kullerud, G.; Yund, R. A.; Moh, G. H. Phase relations in the Cu-Fe-S, Cu-Ni-S and Fe-Ni-S system. In H. D. B. Wilson (ed.) Magmatic Ore Deposits, Vol. 4. Econ. Geol. Monogr., Society of Economic Geologists, Littleton, CO, 1969, 323– 343.
48. Tsujimura, T.; Kitakaze, A. New phase relations in the Cu-Fe-S system at 800°C: constraint of fractional crystallization of a sulfide liquid. *Neues Jahrb. Mineral.* **2004**, *10*, 433– 444.
49. Bayer, G.; Wiedemann, H.G. Thermal analysis of chalcopyrite roasting reactions. *Thermochim. Acta* **1992**, *198*, 303-312.
50. Tkáčová, K.; Baláž, P. Reactivity of mechanically activated chalcopyrite. *International J. Miner. Proc.* **1996**, *44*, 197-208.
51. Tkáčová, K.; Baláž, P.; Bastl Z. Thermal characterization of changes in structure and properties of chalcopyrite after mechanical activation. *Thermochim. Acta* **1990**, *170*, 277-288.
52. Aneesuddin, M.; Char, P.N.; Hussain, M.R.; Saxena, E. R. Studies on thermal oxidation of chalcopyrite from Chitradurga, Karnataka State, India. *J. Therm. Anal.* **1983**, *26*, 205–215.
53. Vaziri, S.; Yalon, E.; Rojo, M.M.; Suryavanshi, A.V.S.; Zhang, H.; McClellan, C.J.; Bailey, C.S. et al., Ultrahigh thermal isolation across heterogeneously layered two-dimensional materials. *Sci. Adv.* **2019**, *5*, eaax1325.